02 NE 075

REPORT DOCUMENTATION PAGE

AFRL-SR-AR-TR-04-

0262

1. REPORT DATE (DD-MM-YYYY)	2. REPORT TYPE	3. DATES COVERED (From - To)
15 August 2002	Final Report	08/01/2002 - 12/31/2003

4. TITLE AND SUBTITLE
Optical Properties of III-V Semiconductor Nanostructures and Quantum Wells

5a. CONTRACT NUMBER

5b. GRANT NUMBER
F49620-02-1-0299

5c. PROGRAM ELEMENT NUMBER

6. AUTHOR(S)
Omar Manasreh

5d. PROJECT NUMBER

5e. TASK NUMBER

5f. WORK UNIT NUMBER

7. PERFORMING ORGANIZATION NAME(S) AND ADDRESS(ES)

Department of Electrical Engineering
3217 Bell Engineering Center
University of Arkansas
Fayetteville, AR 72701

8. PERFORMING ORGANIZATION REPORT NUMBER

9. SPONSORING / MONITORING AGENCY NAME(S) AND ADDRESS(ES)
Air Force Office of Scientific Research
4015 Wilson Boulevard, Room 713
Arlington, VA 22203-1954

10. SPONSOR/MONITOR'S ACRONYM(S)
AFOSR/NE

11. SPONSOR/MONITOR'S REPORT NUMBER(S)

12. DISTRIBUTION / AVAILABILITY STATEMENT
Unlimited

DISTRIBUTION STATEMENT A
Approved for Public Release
Distribution Unlimited

13. SUPPLEMENTARY NOTE

20040520 055

14. ABSTRACT

We have investigated the interband and intersubband transitions in III-V semiconductors quantum wells and quantum dots. We also investigated intersubband transitions III-nitride multiple quantum wells grown of sapphire substrate. In particular, intersubband transitions in InGaAs/GaAs multiple quantum dots and GaN/AlGaN multiple quantum wells. Polarization effect on the phonon modes in GaN/AlGaN heterojunctions field effect transistors were also reported. The final report contains detail discussions of the results obtained during the last 18 months. At the end of the report, we listed our professional activities including technical papers, books, symposia, invited talks, and students supported by the grant.

15. SUBJECT TERMS
Intersubband transitions, Long Wavelength Infrared Detectors, Optoelectronic Materials and Devices, III-V Quantum Wells and dots.

16. SECURITY CLASSIFICATION OF:			17. LIMITATION OF ABSTRACT	18. NUMBER OF PAGES	19a. NAME OF RESPONSIBLE PERSON
a. REPORT	b. ABSTRACT	c. THIS PAGE			19b. TELEPHONE NUMBER (include area code)
Unclassified	Unclassified	Unclassified	None		Omar Manasreh (479) 575-3009

FINAL REPORT

OPTICAL PROPERTIES OF III-V SEMICONDUCTOR NANOSTRUCTURE AND QUANTUM WELLS.

AFOSR Grant number F49620-02-1-0299

Prepared by

Dr. Omar Manasreh
Department of Electrical Engineering, 3217 Bell Engineering Center
University of Arkansas, Fayetteville, AR 72701
Phones: Office: (479)575-3009, FAX: (479)575-7967, E-Mail:
manasreh@engr.uark.edu

Submitted to

LtCol Todd D. Steiner, PhD
Program Manager, Optoelectronic Materials Physics and Electronics Directorate
Air Force Office of Scientific Research
4015 Wilson Boulevard, Room 713, Arlington VA 22203-1954
Phone: 703 696 7314, Fax 703 696 8481
email: todd.steiner@afosr.af.mil

TABLE OF CONTENTS

1. Optical absorption of intersubband transitions in $In_{0.3}Ga_{0.7}As/GaAs$ multiple quantum dots.

Fourier-transform infrared spectroscopy technique was employed to investigate the optical absorption coefficient of intersubband transitions in Si-doped $In_{0.3}Ga_{0.7}As/GaAs$ multiple quantum dot structures. Waveguides with 45° polished facets were fabricated from molecular beam epitaxy grown wafers with different quantum dot size. The measured maximum optical absorption coefficient was found to be in the order of $1.10x10^4 cm^{-3}$. The peak position energy of the intersubband transition was observed to shift toward lower energy when the quantum dot size is increased as expected. The photoluminescence spectra were also measured for different samples with different quantum dot size. The internal quantum efficiency was estimated to be in the order of 58% for a sample with 40 periods of 6nm dot size.

Quantum dots are currently attracting much attention for their application as lasers and detectors as well as for their unique underlying physical properties. For example, one rather attractive application makes use of intersubband transitions in quantum dot structures for long wavelength infrared detection. The quantum dot nanostructure offers a unique solution to the polarization problem that is encountered when using quantum wells to engineer long wavelength infrared detectors. That is, one significant drawback to the use of multiple quantum wells for detectors based on intersubband transitions is that the absorption of normal incident photons is forbidden. Due to the dipole selection rules associated with the intersubband transitions, the incident photons must have a component (TM) of polarization normal to the structure interfaces to excite intersubband transitions and be absorbed. Typically, this requirement has been met by illuminate the sample at the Brewster's angle, polarizes the light with p-polarized light, or adding a grating layer at the top of the detector structure. Using intersubband transitions in quantum dots, where the selection rules allow normal incident light to effectively couple with intersubband transitions, can remove this complication.

The results for long wavelength infrared detectors fabricated from quantum dots are usually expressed in terms of photocurrents (see for example Refs.1-5) and/or photoresponse (see for example Refs. 6-10). While there are extensive theoretical calculations (see for example refs. 11- 21) on the optical absorption coefficient in quantum dots, the reported experimental measurements are scarce and in some cases the absorbance measurements are indistinguishable from the back-ground noise.[22] In this section, we report on the measurements of the optical absorption coefficient of the intersubband transitions in Si-doped $In_{0.3}Ga_{0.7}As/GaAs$ multiple quantum dot structures. The peak position energies of the intersubband transitions of these samples were in the 9 to11 μm spectral range for quantum dot size of 4 to 7 nm. The $In_{0.3}Ga_{0.7}As/GaAs$ quantum dot structures were grown by a solid-source molecular beam epitaxy system on semi-insulating (100) GaAs substrate. A typical structure consists of a 0.5 μm thick Si-doped GaAs buffer layer followed by 40-periods of Si-doped $In_{0.3}Ga_{0.7}As$ dots and 30 nm undoped GaAs barrier. The structure is then capped by a 0.5 μm thick Si-doped GaAs layer. The quantum dot layers are usually doped with $[Si]\sim 1.7\times10^{18}$ cm^{-3}. The growth temperature of $In_{0.3}Ga_{0.7}As$ /GaAs multi-layers was 500 °C with background arsenic pressure of 1×10^{-5} Torr. Several samples were grown with quantum dot diameter in the range of 4 nm - 7 nm. Three samples were chosen for the present study with quantum dot

size of 4, 6, and 7 nm. A high-resolution x-ray diffraction experiment was performed on the samples to confirm their thicknesses. The optical absorption coefficient and the PL spectra were recorded using a BOMEM DA8 spectrometer in conjunction with continuous flow cryostat. The samples were cut into a waveguide geometry with the facet being polished at 45°. The light beam was zigzagged across the width (w) of the sample, which was typically 1.5 mm. The sample thickness (d) including the substrate and the quantum dot structure is in the order 0.35mm. Thus, the number of passes (P) for the present waveguides is $P = w/[d \times \tan(57)] \approx 3$.

In Fig. 1.1 we plotted the optical absorption coefficient, measured at 77K, of the intersubband transitions in three different multiple quantum dot structures. The optical absorption coefficient spectrum of the 7nm sample was multiplied by a factor of 2 for comparison reasons. As expected, the peak position energy of the intersubband transition is red-shifted as the quantum dot size is increased. The spectral shape of the optical absorption coefficient for the samples with quantum dot size of 6 and 7 nm is symmetrical, which indicates a good uniformity of the quantum dot size. However, the

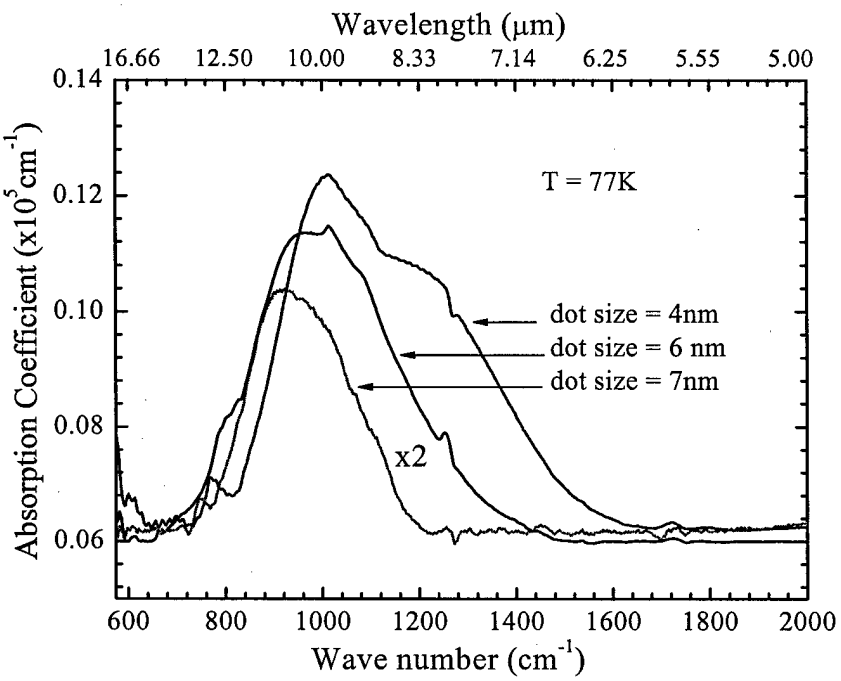

Fig. 1.1. *The optical absorption coefficient spectra of the intersubband transitions in Si-doped $In_{0.3}Ga_{0.7}As/GaAs$ multiple quantum dots measured at 77K were plotted for three different samples with dot size of 4, 6, and 7 nm.*

spectral shape of the sample with a quantum dot size of 4 nm is asymmetrical. This could be explained by the fact that for this sample, there was a growth interruption and we expected to obtain a different growth rate for part of the quantum dot layers. Hence, the variation of the quantum dot size manifests itself in the asymmetrical line shape of the optical absorption coefficient spectrum. The peak position energies of the intersubband

transitions reported in Fig. 1 indicate that the quantum dot structures are suitable for long wavelength infrared detectors in the spectral range of 9 – 11 μm. The full-width-at-half-maximum of the spectra in this figure is much larger than that of the typical intersubband transition spectra in multiple quantum wells, which makes the quantum dot structure useful for broadband detectors.

The photoluminescence (PL) spectra were also recorded for the three samples and are shown in Fig. 1.2. As expected, the interband transitions are blue-shifted as the quantum dot size is decreased. This is demonstrated in the peak position shift of the PL spectra as shown in Fig. 1.2. The full-width-at-half-maximum of the PL spectra is approximately the same for the three samples, which is about 650 cm^{-1} (80.6 meV).

The optical absorption coefficient spectrum for the sample with the quantum dot size of 6nm shows a fine structure with extra small peaks around 780, 1020, 1090, and 1256 cm^{-1}. To investigate the origin of these peaks, we have grown an undoped sample with a structure similar to the 6 nm doped sample. The optical absorption coefficient spectra of both samples are plotted in Fig. 3. It is clear from this figure that the fine structure is present in the undoped sample and therefore this structure is not generated from the quantum dots. We believe that the origin of this structure is from a phase correction problem inherited in the spectrometer due to the non-repeatability of the

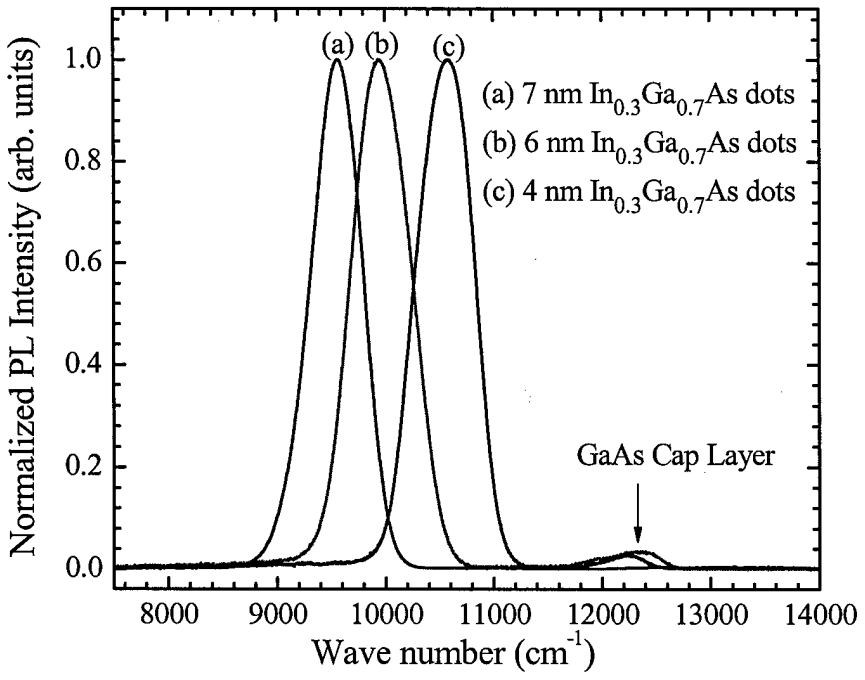

Fig. 1.2. *Photoluminescence spectra measure at 77K for three Si-doped $In_{0.3}Ga_{0.7}As/GaAs$ multiple quantum dot samples with dot size of 4, 6, and 7nm.*

aperture size. Another important observation from Fig. 1.3 is that the intersubband transition is below the detection limit in the undoped sample. However, as has been observed[3], it is quit possible that the intersubband transition of the quantum dot detector could be populated with electrons when a bias voltage is applied during the photocurrent and/or photoresponse measurements.

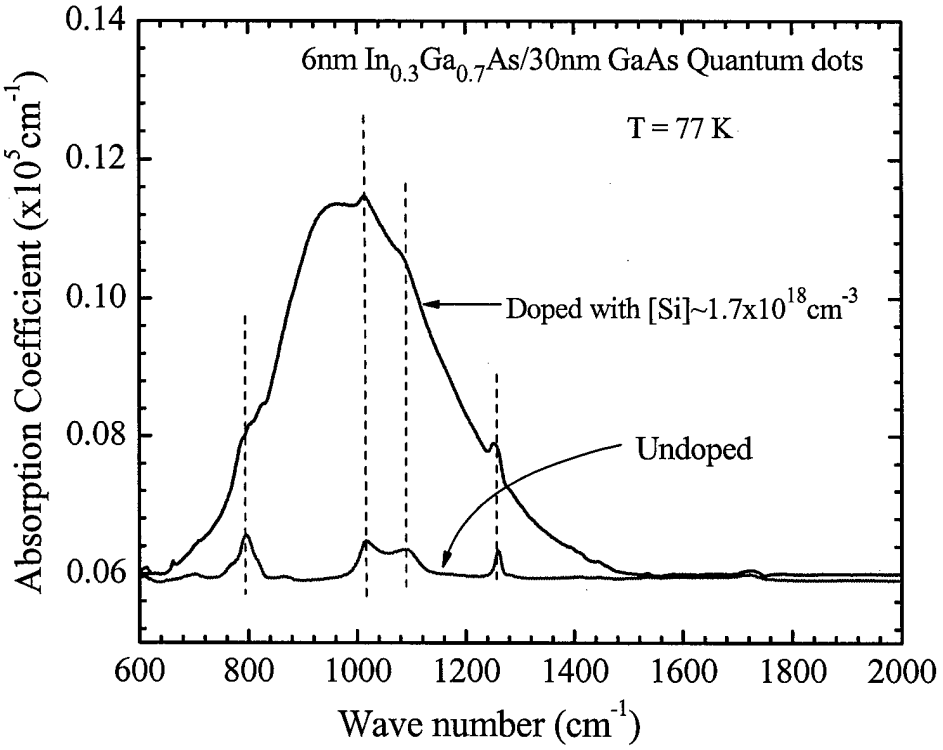

Fig. 1.3. *The optical absorption coefficient spectra of the intersubband transitions in two identical Si-doped and undoped $In_{0.3}Ga_{0.7}As/GaAs$ multiple quantum dot samples measured at 77K. The quantum dot size in both samples was 6 nm.*

The optical absorption coefficient is very important in calculating many detector parameters. For example, the internal quantum efficiency, η_o, can be defined as the fraction of the incident intensity (I_i) that is absorbed by the intersubband transition in the multiple quantum dots, which can be written as[23]

$$\eta_o = (I_i - I_{tn}) / I_i \qquad (1)$$

Where $I_{tn} = I_i(1-\zeta)^{N.P}$, N is the number of the quantum dot layers, P is the number of passes in the waveguide configuration, and ζ is the fractional absorption per quantum dot layer. Thus Eq. (1) can be rewritten as

$$\eta_o = \left\{1 - (1-\zeta)^{N.P}\right\} . \qquad (2)$$

ζ is related to the maximum absorbance (A_{max}) according the following relationship: $A_{max} = -\log_{10}[(1 - \zeta)^{N.P}]$. It should be pointed out that the absorbance is not the absorption coefficient. As a first approximation, the absorption coefficient can be obtained by dividing the absorbance by the total thickness (l) of the active region. In this case, l = N x P x t, where t is the quantum dot layer thickness. With the measured value of A_{max} = 0.383, N=40, and P=3 for the 6nm sample, one finds $\zeta = 7.322 \times 10^{-3}$. For this value, the quantum efficiency, using Eq. (2), is calculated to be 58.6%. Similarly, the quantum efficiency is also calculated as 49.5% and 33.5% for the 4 and 7nm quantum dot size samples, respectively. The internal quantum efficiency expressed in Eq. (2) can thus be reduced to ζ for N=P=1. The internal quantum efficiency calculated here is not exactly the actual detector quantum efficiency (η). But the relationship between them[24] can be expressed as $\eta = \eta_o P_e$, where P_e is the probability that a photoexcited carrier will escape from the quantum dot and contribute to the photocurrent rather than be recaptured by another quantum dot.

In order to compare the 6 nm quantum dot structures to a regular multiple quantum well structure (MQWs), we tested a MQW sample of 50 periods 7.5 nm GaAs/10 nm $Al_{0.3}Ga_{0.7}As$ MQWs. The GaAs quantum well was nominally doped with [Si]~$2 \times 10^{18} cm^{-3}$. The waveguide was constructed with the same dimension as the waveguides fabricated from the quantum dots sample. The absorbance of the intersubband transition in the MQWs was A_{max}=0.392, which is comparable to the absorbance measured for the 6 nm multiple quantum dots sample. Using Eq. (2), and $A_{max} = -\log_{10}[(1 - \zeta)^{N.P}]$, we calculated η_o to be 59.4% for the 50 period MQWs. However, by normalizing A_{max} for the MQWs to 40 periods instead of 50 periods, η_o is reduced to 51.4%, a slightly smaller value than that of the corresponding quantum dot structure measured at 58.6%

In conclusion, the optical absorption coefficient of the intersubband transitions in the spectral range of 9 – 11 μm for molecular beam apitaxy grown $In_{0.3}Ga_{0.7}As/GaAs$ multiple quantum dot layers was investigated as a function of quantum dot size. The values of the optical absorption coefficient were measured to be in the order of $1.10 \times 10^4 cm^{-1}$. The broad spectra reported in this study show that these structures are also useful in broadband infrared detector applications. The internal quantum efficiency was estimated to be in the order of 58% for the best samples investigated here, which is comparable, if not better than the quantum efficiency obtained for the multiple quantum wells.

2. Infrared optical absorbance of intersubband transitions in GaN/AlGaN multiple quantum well structures.

Intersubband transitions in Si-doped molecular beam epitaxy grown GaN/AlGaN multiple quantum wells on c-plane sapphire were investigated using Fourier-transform infrared optical absorption technique. Several GaN quantum well samples were grown with either AlGaN bulk or GaN/AlGaN short period superlattice barriers. The measurements were made in a waveguide configuration utilizing a facet polished at 45° to the c-plane. The integrated area of the intersubband transitions in several waveguides cut from different location of the wafer was measured and from which we estimated the two-dimensional electron gas (2DEG) density (σ). The measured values of σ are about two

orders of magnitude larger than the Si doping level of ~$8x10^{17}cm^{-3}$, which is consistent with polarization effects particularly considering the large number of GaN/AlGaN interfaces. The internal quantum efficiency of the intersubband transitions was estimated to be in the order of 40% for samples with superlattice barriers.

III-nitride materials have attracted tremendous interest for their applications to ultraviolet, Blue/green diode lasers and LEDs, high temperature electronics, high-density optical data storage, and electronics for aerospace and automobiles.[25-27] While most of the applications of III-nitride materials lie in the visible and ultraviolet spectral region, there has been increasing interest in this class of materials for the infrared spectral region.[28-32] This interest stems from the fact that GaN/AlGaN system exhibits a large conduction band offset (up to 1.7 eV for AlN barrier) that allow one to optically design structures with intersubband transitions in the wavelength region spanning 0.7 – 14 μm. Additionally, the intersubband transition relaxation time in GaN/AlGaN was predicted theoretically[33-35] to be 100 fs (see also Ref. 32) at 1.55 μm, which is one order of magnitude shorter than the relaxation time in InGaAs multiple quantum wells.[36]

In this section, we report on the optical absorbance of the intersubband transitions in Si-doped GaN/AlGaN multiple quantum wells grown by molecular beam epitaxy (MBE). The total integrated area of the intersubband transitions was measured. The two-dimensional electron gas (2DEG) density was calculated from the total integrated area and found to be about two orders of magnitude larger than expected from the Si-doping level of ~$8x10^{17}cm^{-3}$. Thus, the polarization-induced electrostatic charge formed at the GaN/AlGaN interfaces is the dominant factor in the formation of the large values of 2DEG density in the quantum wells. The internal quantum efficiency of the intersubband transitions was estimated to be in the order of 40% for most of the samples with superlattice barriers.

The GaN/AlGaN multiple quantum well structures were grown on *c*-plane sapphire (Al_2O_3) substrates using an MBE system with rf-plasma N_2 as active nitrogen source. The 2 inch substrate was not rotated during the growth, which resulted in nonuniform growth. An initial AlN buffer layer of ~50 nm was grown on nitiridated Al_2O_3 substrate as a template for the subsequent epilayers. The growth parameters thus chosen consistently lead to Ga polarity film. Three wafers denoted A, B, and C were chosen for the present study. The GaN quantum wells in the three samples were doped with [Si] ≈$8x10^{17}cm^{-3}$. Wafer "A" consists of a buffer, which is made of 500 Å AlN followed by 0.5 μm GaN, and 50 periods of 35 Å GaN/ 100 Å $Al_{0.35}Ga_{0.65}N$ multiple quantum wells (MQWs) were grown. A cap layer of 300 Å GaN was then grown at the top of the quantum well structure. Wafer "B" consists of a buffer layer similar that of sample "A" and 50 periods of the well/barrier structure. The well is 27.7 Å doped GaN and the barrier is made of four periods of 10Å Si-doped GaN/15Å $Al_{0.65}Ga_{0.35}N$. Wafer "C" consist of 540Å AlN and 1.33 μm Si-doped $Al_{0.50}Ga_{0.50}N$ buffer layer followed by 50 periods of well/barrier structure. The well is 13Å GaN and the barrier consists of four periods of 5Å Si-doped GaN/10Å $Al_{0.65}Ga_{0.35}N$. The cap layer of this wafer was 10 Å $Al_{0.65}Ga_{0.35}N$. The optical absorbance measurements were recorded using a BOMEM DA8 spectrometer in conjunction with continuous flow cryostat. The samples were cut into waveguide geometry with the beveled facet having been polished at 45°. The light beam was zigzagged across the width (w) of the sample, which was typically 2.5 mm. The sample thickness (d) including the substrate and the quantum well structure is on the

order of 0.43mm. Thus, the number of passes (P) for the present waveguides is P = w/[d x tan(69.6)] ≈2 assuming that the refractive index of the sapphire substrate is 1.7.

In Fig. 2.1, we show the absorbance of the intersubband transitions as a function of wavelength for the three waveguide samples, which were cut from the center of each of the three wafers. The fine structure observed around 3.4 μm is due to C-H local vibrational modes.[37] The intersubband transition spectra in this figure indicates that the

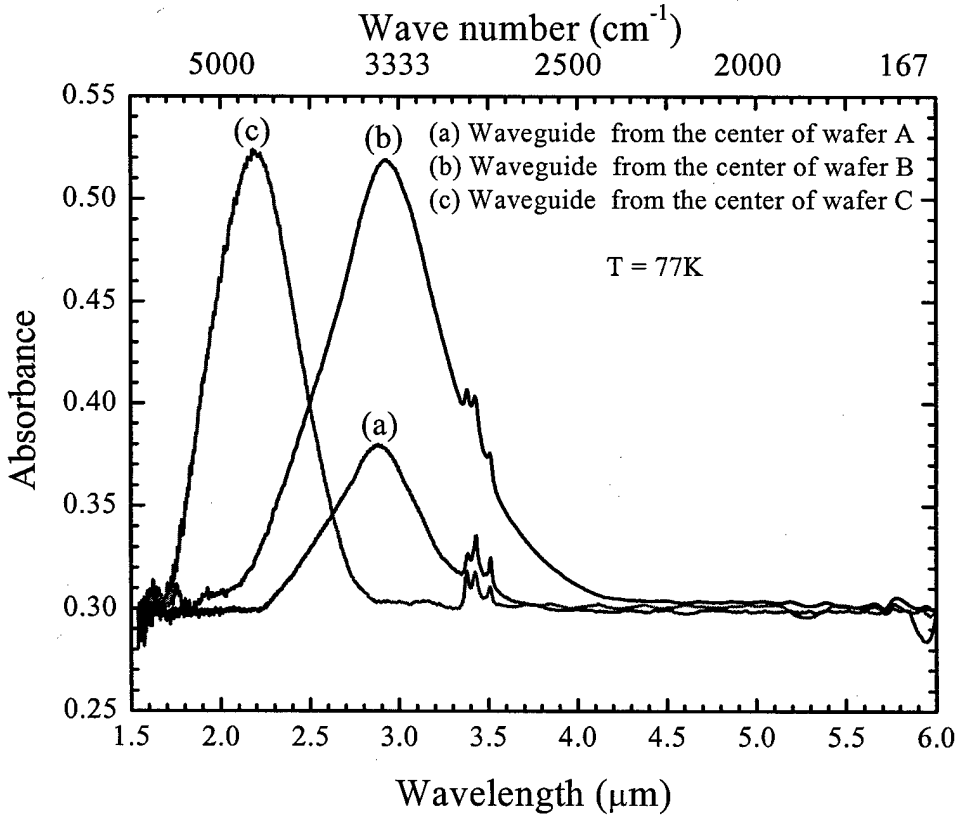

Fig. 2.1. *Absorbance spectra of intersubband transitions measured at 77K for three waveguides cut from identical locations (center) of GaN/AlGaN multiple quantum well wafers.*

peak position energy is blue shifted toward higher energies as the well width is decreased from 27.7Å (sample B) to 13Å (sample (C). However, the intersubband transition in sample (A), which has a well width of 35Å is very close to that of sample B. This indicates that due to the no-uniformity of the wafers, the actual well thickness of both samples A and B is almost the same.

The uniformity of the wafers was investigated by cutting several waveguides from each wafer and then run the absorbance measurements for each waveguide. Some of the results are shown in Fig. 2.2. The intersubband transition spectra in Fig. 2.2 were recorded for a sample (cut from the center of wafer B) measured at the Brewster's angle configuration, spectrum (a), and for four waveguides cut from the center [spectra (b) and (c)], middle, spectrum (d), and edge, spectrum (f), of wafer B. It is clear from Fig. 2.2

that the peak position energy of the intersubband transition is almost the same for the waveguides cut from the center of the wafer [see spectra (b) and (c)] but it is blue-shifted (shorter wavelength) for the waveguide that was cut half way between the center and the edge (we refer to this piece as the middle waveguide) of the wafer [see spectrum (d)]. The shift can be explained in terms of the reduction of the well thickness. However,

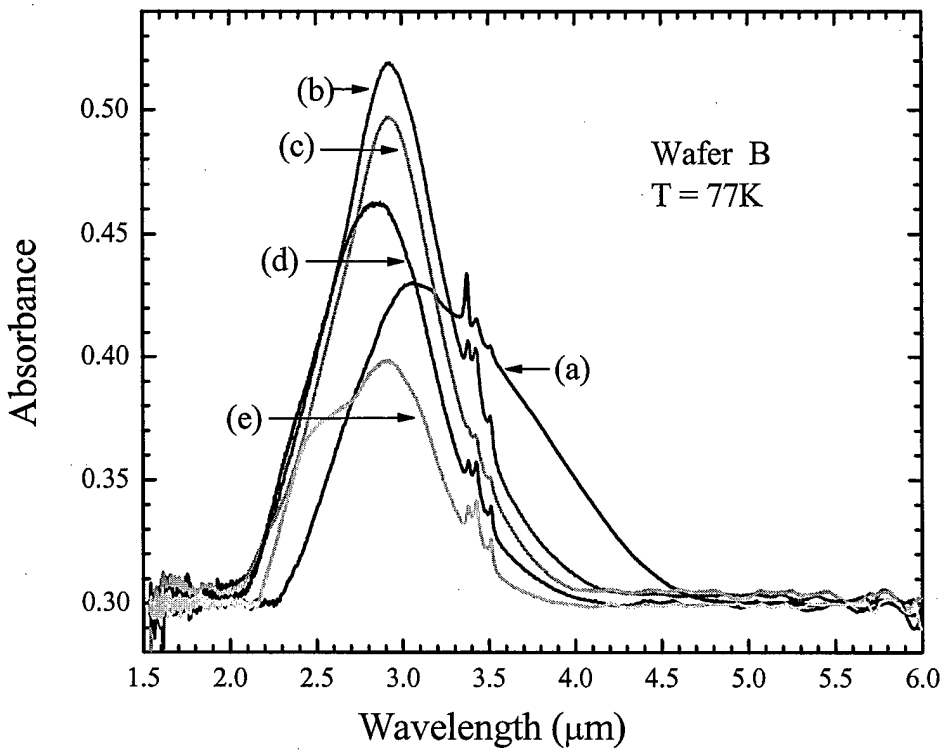

Fig. 2.2. Several absorbance spectra of intersubband transitions measured for waveguides cut from wafer B. Spectrum (a) was measured at the Brewster's angle for a sample cut from the center of the wafer. The rest of the spectra were measured for waveguides cut from (b) the center, (c) off-center, (d) middle, and (e) edge of the wafer. The "middle" is half way between the center and the edge of the wafer.

spectrum (e) which was measured for a waveguide that was cut from the edge of the wafer shows two peaks. This indicates that there are two dominant well thicknesses of the 50 quantum wells. Moreover, the intensity of the peak is reduced for waveguides cut from the middle and the edge of the wafer. Another observation in Fig.2.2 is that the peak position energy of the intersubband transition measured for the waveguides is blue-shifted as compared to the peak position energy measured at the Brewster's angle. This however is opposite to the trend rep0rted for GaAs MQWs.[38-39], but in agreement with the multiple quantum dot measurements.[40]

The total integrated area (I) of the intersubband transition can be related to the 2DEG density (s) according to the following relationship:[41]

$$I \approx \frac{PNb\ \sigma L e^2 h}{4\varepsilon_o m^* c} \frac{f}{n^2(n^2+1)^{1/2}}, \quad (1)$$

where, P is the number of passes in the waveguide, N is the periods of quantum wells, in this case 50, b is the number of the interfaces per period that contribute polarization-induced sheet charges (b is taken as 1 for wafer A and 5 for wafers B and C), σ is the 2DEG density, L is the well thickness, e is the charge of the electron, h is Planck's constant, ε_o is the permittivity of space, m* is the electron effective mass, c is the speed of light, n is the refractive index of the quantum well material, and *f* is the oscillator strength which is taken as $0.96m_o/m^*$ for the ground state to the first excited state transition.[41] From Eq. (1) one can estimate σ and the results are shown in table I for the three spectra shown in Fig. 1.

The Fermi energy level (E_F) is also estimated using the following expression: $\sigma_{3D} = 2\left(\frac{2\pi m^* kT}{h^2}\right)^{3/2} e^{(E_F - E_c)/kT}$, where k is Boltzmann constant, T is the temperature, σ_{3D} is the three-dimensional electron density, and E_c is the bottom of the conduction band. The results are shown in table 2.1I, where (E_F-E_c) is calculated for both 77 and 300K. From the calculated E_F and the measured intersubband transition energies, it is determined that the Fermi Energy level lies between the ground and the first excited states for both 77 and 300K.

Table 2.1: *The well width, the doping level, the 2DEG density estimated from Eq. (1), and the Fermi energy level (E_F) with respect to the bottom of the conduction band (Ec) are listed for the samples shown in Fig. 2.1.*

Wafer	Well width (Å)	[Si] ($x10^{11}cm^{-2}$)	σ ($x10^{13}cm^{-2}$)	(E_F-Ec) (eV)	
				77K	300K
A	35	2.80	6.93	0.0761	0.244
B	27.7	2.22	5.83	0.0856	0.281
C	13	1.04	15.50	0.0921	0.306

From table 2.1, it is clear that the Si-doping level cannot alone account for the high 2DEG density estimated from the integrated area of the intersubband transitions. One plausible explanation for the high σ values is that the polarization-induced electrostatic sheet charges at the GaN/AlGaN interfaces[42-46] contribute most of the electrons in the well. This premise is supported by the fact that a single interface exists in wafer A (bulk barrier), while there are 5 interfaces per period (one comes from the quantum well and four come from the superlattice barrier) in wafers B and C. Figure 1 shows a clear evidence that the intensity of the intersubband transition for wafer A is much smaller than that of the intersubband transitions in wafers B and C. Hence Eq. (1) was modified by adding the interface factor, b.

The internal quantum efficiency, η_o, for the three samples was calculated from the absorbance spectra in Fig. 1 according to the following relationship:[47]

$$\eta_o = (I_i - I_{tn})/I_i = [1-(1-\zeta)^{N.P.b}], \quad (2)$$

where I_i is the incident light intensity, $I_{tn} = I_i(1-\zeta)^{N.P.b}$, N=50, P=2, b=1 for wafer A and 5 for wafer B and C, and ζ is the fractional absorption per quantum well. ζ is related to the maximum absorbance (A_{max}) according the following relationship: $A_{max} = -\log_{10}[(1 - \zeta)^{N.P.b}]$. With the measured values of A_{max} = 0.0795, 0.218, and 0.222 for the three spectra in Fig. 1, one finds ζ=1.823x10^{-3}, 1.003x10^{-3}, 1.021x10^{-3}, for spectra (a), (b), and (c), respectively. For these values, the quantum efficiency is calculated to be 16.70%, 39.50%, and 45.40% for the three spectra (a), (b), and (c) in Fig. 1, respectively.

In conclusion, the infrared absorbance measurements of the intersubband transitions in GaN/AlGaN multiple quantum wells are reported for samples with either bulk or short period superlattice barriers. The two-dimensional electron gas density formed in the quantum wells was estimated from the total integrated area of the intersubband transitions and found to be at least two orders of magnitude larger than the intentional Si-doping level. The large electron density is attributed to the polarization-induced sheet charges formed at the GaN/AlGaN interfaces. This assertion was confirmed by the observation of the low (high) value of the integrated area of intersubband transition in samples with AlGaN bulk (GaN/AlGaN superlattice) barriers. The internal quantum efficiency was estimated for the intersubband transition and it was found that samples with superlattice barriers possess higher quantum efficiency as compared to samples with bulk AlGaN barriers.

3. Photoluminescence of metalorganic chemical vapor deposition grown GaInNAs/GaAs single quantum wells

Photoluminescence (PL) spectra of interband transitions in GaInNAs/GaAs single quantum wells grown by metalorganic chemical vapor deposition technique on semi-insulating GaAs substrates were measured at 77 K for several samples grown with different In composition and dimethylhydrazine (DMH)/III ratios. The results show that the PL intensity increases as the In mole fraction is increased from 0 to 25%, but the PL intensity is degraded for samples with an In mole fraction of 30% or higher. The peak position energies of the PL spectra were investigated as a function of the DMH/III ratio. Thermal annealing effect induced a blue-shift in the PL spectra peak position energy in samples grown with high DMH/III ratio.

Diluted or small band gap nitrides semiconductors such as GaInNAs and GaNAs are currently being investigated for their optoelectronic applications such as 1.3 and 1.55 μm emitters used for optical communication. Devices based on this class of materials possess advantages over other material systems. For example, the higher temperature characteristic GaInNAs/GaAs lasers provides an advantage over the GaInPAs/InP lasers. The InGaNAs/GaAs system has a larger conduction band offset, which provides a higher quantum confinement.[48] The GaInNAs-based systems is grown on GaAs substrate which is more robust substrates as compared to the InP substrates. Bragg reflectors are easy to fabricate for GaInNAs/GaAs vertical cavity surface emitting lasers compared to GaInPAs/InP Bragg reflectors.[49] The investigation of GaInNAs/GaAs system was motivated by the fabrication of light emitters that can cover the entire visible spectral

range based on the direct band-gap materials. Recently, emission was observed in GaInNAs/GaAs quantum wells (see for example Refs. 50-54) and quantum dots (see for example Refs. 55-57). Thermal annealing effect on the photoluminescence spectra was also investigated by various groups (see for example Refs. 51, 58-61). From various reports on the growth and characterization of the InGaNAs/GaAs system, it is realized that nitrogen incorporation leads to a number of properties that were found to be attractive for device applications.

In this section, we report on the photoluminescence (PL) of GaInNAs/GaAs single quantum wells grown on semi-insulating GaAs substrates. The PL spectra were investigated at 77K as a function of In composition, dimethylhydrazine (DMH)/III ratios, and thermal annealing. The PL intensity, full width at half maximum, and the peak position energy were all found to strongly depend on the incorporation of In and N atoms.

The structures were grown by atmospheric-pressure metalorganic vapor phase epitaxy at 570 °C on semi-insulating GaAs oriented 2 degrees from (100) to (110). Trimethylgallium, trimethylindium, arsine, and dimethylhydrazine (DMH) were used as precursors. The growth rate was 5 microns/h for the GaInNAs active layers. The N content was changed for the various samples by varying the DMH source flow rate. As described by the quantity DMH/III, the ratio of DMH to group-III flows injected into the reactor. The GaInNAs active layers were 100 Å thick, and were cladded on both sides by GaAs doped n-type with silicon from disilane precursor. After the growth of each structure was completed but before it was removed from the reactor, it was annealed under arsine for 30 minutes at 650 °C. A few samples were annealed for 10 minutes at 750 °C under arsine in the metal-organic chemical vapor deposition (MOCVD) reactor. The arsine flow rate during the anneal was 30 standard cubic centimeters per minute (sccm). For comparison, the actual growth of all the original epilayers was done with an arsine flow of 1.9 sccm. Additional samples were annealed at 800 °C with no arsine, but with a GaAs wafer lying face-down on the epilayer as a proximity cap. The InGaAs/GaAs single quantum well samples were grown on semi-insulating GaAs substrates in a molecular beam epitaxy (MBE) chamber. The Growth temperature was 585 °C and the samples were post-growth annealed at 600 °C for 10 minutes. The PL spectra were recorded using BOMEM DA8 spectrometer in conjunction with continuous flow cryostat.

Photoluminescence spectra obtained for several samples are shown in Fig. 3.1. The In mole fraction was fixed for all nine samples, shown in the figure, at 7% while the DMH/III ratio varied as shown in the inset. Sample number 1 does not contain any N (DMH/III ratio is zero) and since the conduction band offset is very small in this sample, its PL spectrum is very weak due to the low quantum confinement. As the N concentration is increased, which is reflected by the increase of the DMH/III ration, the quality of the PL spectra is significantly improved as shown in samples number 2, 3, and 4. The intensity of the PL spectra is degraded as the DMH/III ratio increased above 71. However, the peak position energy of the PL spectra continues to show a red-shift as the DMH/III ratio is increased while the intensity of the PL spectra continues to decrease.

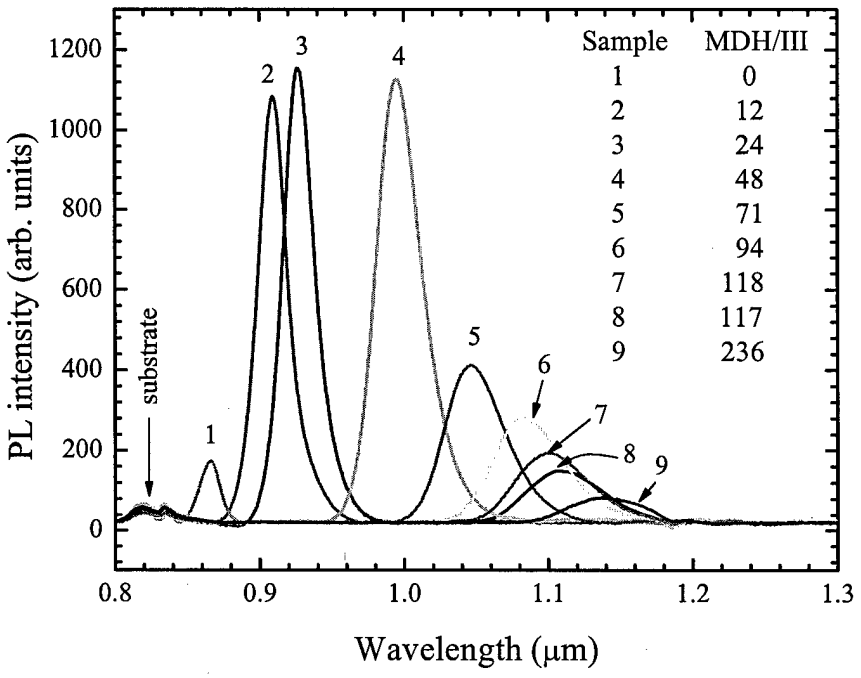

Fig. 3.1. *Photoluminescence spectra obtained at 77K for several $Ga_{0.93}In_{0.07}NAs/GaAs$ single quantum well samples as a function of DMH/III ratio. The inset is a table showing the sample numbers and their MDH/III ratios*

The PL spectra were also investigated as a function of the In mole fraction. Several spectra are shown in Fig. 3.2 for both samples grown by MOCVD and MBE techniques. The N free samples (samples number 10, 11, 12, and 18) were grown by the MBE technique. The inset in this figure is the table that shows the In mole fraction and the DMH/III ratio for the samples. We noted a few observation in this figure. First, the intensity of the PL spectra for the GaInAs samples (MBE samples) is increased as the In mole fraction is increased. This behavior can be understood in terms of the quantum confinement, which is increased as the In mole fraction is increased. Second, the PL spectrum for GaInAs sample number 18 is very week and broad as compared to the PL spectra labeled 10, 11, and 12. This may be due to the degradation of the interfaces (In segregation at the interfaces) as the In mole fraction is increased beyond 25%. Third, the intensities of the PL spectra for the samples that contained N (spectra labeled 13, 14, and 15) are very weak. However, upon increasing the In composition to 30%, the intensities of the spectra are increased as shown in the spectra labeled 16 and 17. The spectra labeled 16 and 17 are taken for the samples that contain 30% In with DMH/III ratios of 47 and 71, respectively. Even though the DMH/III ratio is increased from 47 to 71, the PL spectrum for sample number 17 is only slightly shifted. This behavior strongly suggest that N atoms reached a point that cannot be incorporated any further by increasing the DMH/III ratio. Fourth, the intensities of the PL spectra labeled 16 and 17

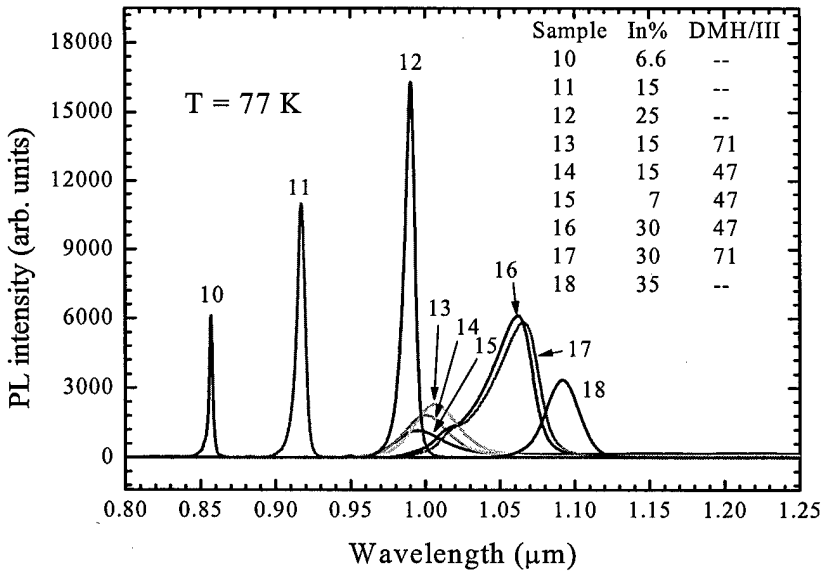

Fig. 3.2. *Photoluminescence spectra obtained at 77K for several GaInNAs/GaAs single quantum well samples as a function of In mole fraction and DMH/III ratio. The inset is a table showing the sample numbers and their In compositions and MDH/III ratios.*

are stronger than those labeled 13, 14, and 15. This indicates that the quality of the samples is improved as the In mole fraction is increased in the GaInNAs single quantum wells.

The peak position energy of the PL spectra for $Ga_{0.93}In_{0.07}NAs/GaAs$ samples was plotted as a function of DMH/III ratio as shown in Fig. 3.3. It is clear from this figure that the data exhibit a large bowing factor as compared to the almost linear behavior of the band gap of InGaAs as a function of In mole fraction.[62] The relative integrated intensity and the full width at half maximum (FWHM) of the PL spectra were also investigated for $Ga_{0.93}In_{0.07}NAs/GaAs$ samples as a function DMH/III ratio. The results are shown in Fig. 3.4. The relative integrated intensity is initially increased and then decreased as a function of the DMH/III ratio. On the other hand, the FWHM is increased with DMH/III ratio and then leveled as the ratio is increased above 100.

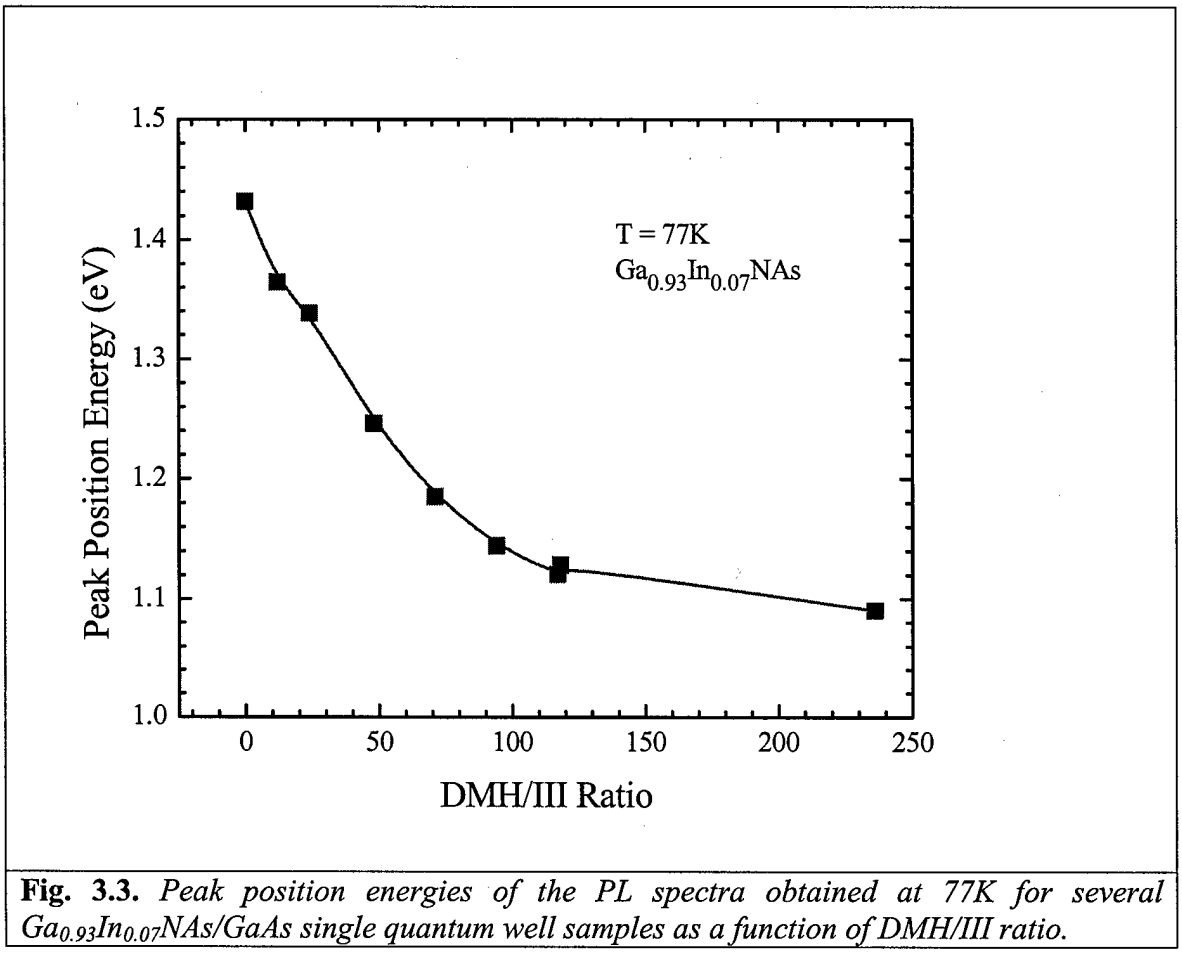

Fig. 3.3. *Peak position energies of the PL spectra obtained at 77K for several $Ga_{0.93}In_{0.07}NAs/GaAs$ single quantum well samples as a function of DMH/III ratio.*

Post growth thermal annealing (either rapid thermal or furnace annealing) studies have shown that the intensity of the PL spectra can be improved when GaInNAs samples are annealed at temperature higher than the growth temperature.[54, 58, 59, 61, 63] On the other hand, the peak position energy of the PL spectra where shown to shift toward higher energies.[51, 54, 56, 58, 59, 61, 63] In the present investigation, we annealed a $Ga_{0.93}In_{0.07}NAs$ sample, grown with a DMH/III ratio of 119, at 750 °C and 800 °C for 10 minutes and the results are shown in Fig. 3.5. The results in this figure indicates that the intensity of the PL spectrum is reduced after thermal annealing at 750 °C and completely washed out after annealing the sample at 800 °C. The broad PL band observed at higher wavelength in the spectra is most likely due to emission from N-N centers formed in the sample. The peak position energy is also blue-shifted in a good agreement with other studies.[51, 54, 56, 59] The blue-shift observed in the PL spectrum of the sample after annealing is perhaps due to degradation of the interfaces that caused by intermixing.

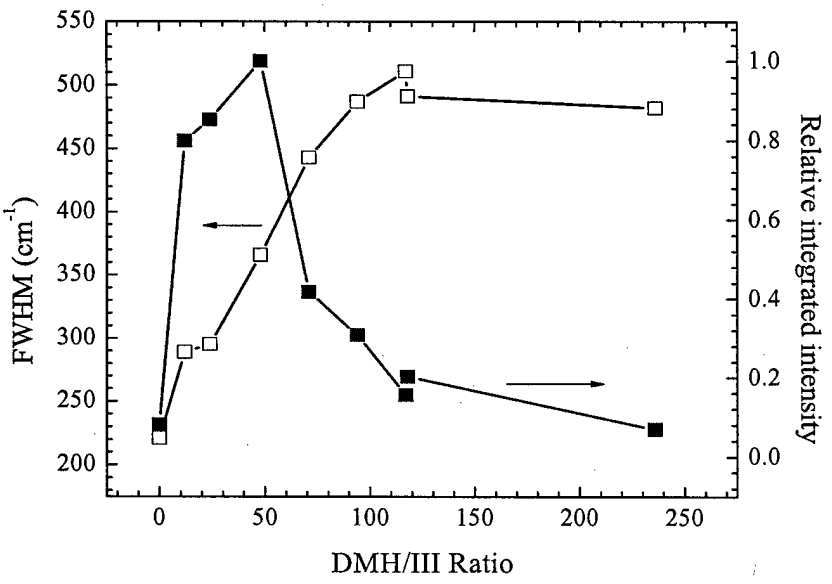

Fig. 3. 4. *The full width at half maximum (FWHM) and the relative integrated intensities of the PL spectra obtained at 77K for several $Ga_{0.93}In_{0.07}NAs/GaAs$ single quantum well samples as a function of DMH/III ratio.*

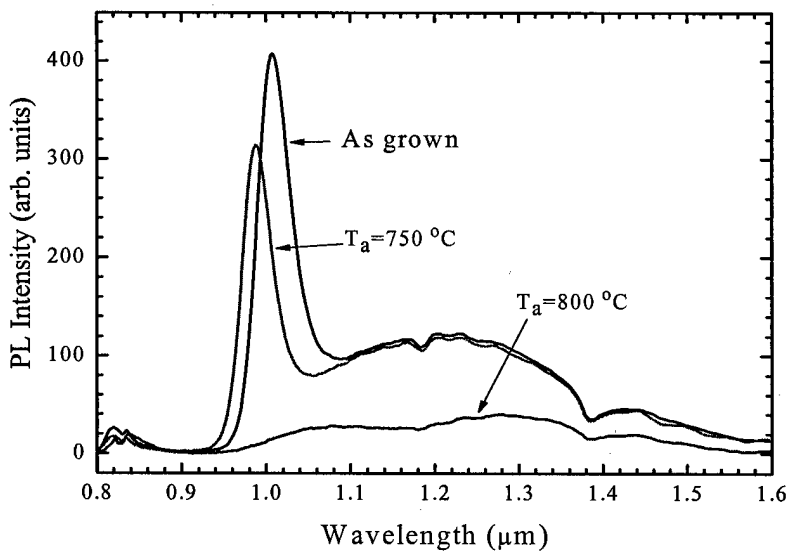

Fig. 3.5. Post growth thermal annealing effect on the PL spectrum of a $Ga_{0.93}In_{0.07}NAs/GaAs$ single quantum well sample grown with a DMH/III ratio of 119. The sample was annealed for 10 minutes at each annealing temperature of T_a=750 °C and 800 °C. The spectra were measured at 77K.

In conclusion, we investigated the PL spectra of various GaInNAs/GaAs single quantum well samples grown under different conditions. The PL intensity is improved as the DMH/III ratio is increased from 0 to about 50 and then starts to decrease as this ratio continues to increase above 50. The quality of the PL spectra was shown to degrade as the N mole fraction, which manifest itself in the DMH/III ratio, is increased. In $Ga_{0.7}In_{0.3}NAs$ samples, the PL intensity and peak position remains the same as the DMH/III ratio is changed from 47 to 71, which indicates that N atoms do not seem to incorporate in a substitutional crystal sites above certain DMH/III ratio. The peak position energy of the PL spectra obtained for a set of $Ga_{0.93}In_{0.07}NAs/GaAs$ samples was investigated as a function of the MDH/III ratio. Post-growth thermal annealing shows that, in addition to the reduction of the intensity, the peak position energy of the PL spectra are blue-shifted.

4. References

1. Z. Ye, J. C. Campbell, Z. Chen, E. –T. Kim, and A. Madhukar, J. Appl. Phys. **92**, 7462 (2002).
2. E. –T. Kim, Z. Chen, M. Ho, and A. Madhukar, J. Vac. Sci. Technol. **B20**, 1188 (2002).
3. Z. Chen, O. Baklenov, E. –T. Kim, I. Mukhametzhanov, J. Tie, A. Madhukar, Z. Ye and J. C. Campbell, J. Appl. Phys. **89**, 4558 (2001).
4. E. –T. Kim, Z. Chen, M. Ho, and A. Madhukar, Appl. Phys. Lett. **79**, 3341 (2001).
5. D. Pan, E. Towe, and S. Kennerly, Appl. Phys. Lett. **75**, 2719 (1999).
6. Z. Ye, J. C. Campbell, Z. Chen, E. –T. Kim, and A. Madhukar, J. Appl. Phys. **92**, 4141 (2002).
7. H. C. Liu, M. Gao, J. McCaffrey, Z. R. Wasilewski, and S. Fafard, Appl. Phys. Lett. **78**, 79 (2001).
8. L. Chu, A. Zrenner, M. Bichler, and G. Abstreiter, Appl. Phys. Lett. **79**, 2249 (2001).
9. S. Maimon, E. Finkman, G. Bahir, S. E. Schacham, J. M. Garcia, and P. M. Petroff, Appl. Phys. Lett. **73**, 2003 (1998).
10. S. Kim, H. Mohseni, M. Erdtmann, E. Michel, C. Jelen, and M. Razeghi, Appl. Phys. Lett. **73**, 983 (1998).
11. B. Krummheuer, V. M. Axt, and T. Kuhn, Phs. Rev. **B 65**, 195313 (2002).
12. A. Vasanelli, R. Ferreira, and G. Bastard, Phys. Rev. Lett. **89**, 216804 (2002).
13. F. Thiele, Ch. Fuchs, R. v. Baltz, Phys. Rev. **B 64**, 205309 (2001).
14. A. D. ANdreev, E. V. Kolokova, and A. A. Lipovskii, J. Appl. Phys. **88**, 750 (2000).
15. A. Franceschetti, A. Zunger, Phys. Rev. **B 62**, R16287 (2000).
16. S. –S. Li, J. –B Xia, Phys. Rev. **B 55**, 15535 (1997).
17. M. A. Cusack, P. R. Briddon, and M. Jaros, Phys. Rev. **B 56**, 4047 (1997).
18. H. Imamura, P. A. Maksym, and H. Aoki, Phys. Rev. **B 53**, 12613 (1996).
19. N. Taniguchi and V. N. Prigodin, Phys. Rev. **B 54**, 14305 (1996).
20. R. W. Hasse, and N. F. Johnson, Phys. Rev. B 49, 14409 (1994).
21. L. M. Ramaniah, and S. V. Nair, Phys. Rev. B 47, 7132 (1993).
22. S. Krishna, O. Qasimeh, P. Bhattacharya, P. J. McCann, and K. Namjou, Appl. Phys. Lett. **76**, 3355 (2000).

23. E. R. Brown, S. J. English, and K. A. McIntosh, in "*Long Wavelength Infrared Detectors*", Vol. 1, Edited by M. Razeghi, (Gordon and Breach, Amsterdam, 1996), chap. 6, p. 335.
24. G. J. Brown and F. Szmulowikz, in "*Long Wavelength Infrared Detectors*", Vol. 1, Edited by M. Razeghi, (Gordon and Breach, Amsterdam, 1996), chap. 5, p. 271.
25 . Morkoç, "*Nitride Semiconductors and Devices.*" (Springer Verlog, Heidelberg, 1999).
26 S. N. Mohammad and H. Morkoç, "*Progress and prospects of Group III-V Nitride Semiconductors.*" Progress in Quantum Electronics **20**, 361 (1996).
27 S. J. Pearton, J. C. Zolper, R. J. Shul, and T. Ren, J. Appl. Phys. **86**, 1, (1999).
28 N. Suzuki and N. Iizuka, Jpn. J. Appl. Phys. **38**, L363 (1999).
29 C. Gmachl, H. M. Ng, and A. Y. Cho, Appl. Phys. Lett. **77**, 334 (2000).
30 C. Gmachl, H. M. Ng, S. -N. George Chu, and A. Y. Cho, Appl. Phys. Lett. **77**, 3722 (2000).
31 K. Kishino, A. Kikuchi, H. Kanazawa, and T. Tachibana, Appl. Phys. Lett. 81, 1234 (2002).
32 N. Iizuka, K. Kaneko, and N. Suzuki, Appl. Phys. Lett. **81**, 1803 (2002).
33 N. Suzuki and N. Iizuka, Jpn. J. Appl. Phys. **36**, L1008 (1999).
34 N. Suzuki and N. Iizuka, Jpn. J. Appl. Phys. **37**, L369 (1998).
35 N. Suzuki and N. Iizuka, in *Physics and Simulation of Optoelectronic Devices VI*, edited by M. Osinski, P. Blood, and A. Ishibashi, Proc. SPIE, Vol **3283**, Pt. 2, P. 614 (1998).
36 T. Asano, K. Tomoda and S. Noda, in Ext. Abstr. 25th Int. Symp. Compound Seicond. (ISCS 1998), Nara Fr1B-1 (1998).
37 M. O. Manasreh, J. M. Baranowski, K. Pakula, H. X. Jiang and Jingyu Lin, Appl. Phys. Lett. **75**, 659 (1999).
38 E. Dupont, M. Gao, H. C. Liu, Z. R. Wasilewski, A. Shen, M. Zaluzny, S. R. Schmidt, and A. Seilmeier, Phys. Rev. **B 61**, 13050 (2000)
39 M. Zaluzny and C. Nalewajko, Phys. Rev. **B 59**, 13043 (1999).
40 B. Pattada, Jiayu Chen, M. O. Manasreh, M. Hussien, W. Ma, and G. J. Salamo, (unpublished).
41 L. C. West, S. J. Eglash, Appl. Phys. Lett. **46**, 1156 (1985).
42 F. Bernardini, V. Fiorentini, and D. Vanderbilt, Phys. Rev. **B 56**, R10024 (1997).
43 E. T. Yu, G. J. Sullivan, P. M. Asbeck, C. D. Wang, D. Qiao, and S. S. Lau, Appl. Phys. Lett. **71**, 2794 (1997).
44 E. T. Yu, in "*III-V Nitride Semiconductors: Applications and Devices*" Vol. 19, edited by E. T. Yu, and M. O. Manasreh, (Taylor and Francis, New York, 2003), Chap. 4, pp. 161-191
45 H. Morkoç, R. Cingolani, and Bernard Gil, "*Polarization Effects in Nitride Semiconductors and Device Structures*", Materials Research Innovations, Vol. 3, No. 2, pp. 97-106, August 1999.
46 H. Morkoç, A. Di Carlo and R. Cingolani, Solid State Electronics, Vol. **46**, Issue 2 pp. 157-202, (2002)
47 E. R. Brown, S. J. English, and K. A. McIntosh, in "*Long Wavelength Infrared Detectors*", Vol. 1, Edited by M. Razeghi, (Gordon and Breach, Amsterdam, 1996), chap. 6, p. 335.
48. M. Kondow, K. Uomi, A. Niwa, T. Kitatani, S. Watahiki, and Y. Yazawa, Jpn. J. Appl. Phys. Part 1, **35**, 1273 (1996).

49. T. Takeuchi, Y. –L. Chang, A. Tandon, D. Bour, R. Twist, M. Tan, and H. –C. Luan, Appl. Phys. Lett. **80**, 2445 (2002).
50. N. Y. Li, C. P. Hains, K. Yang, J. Lu, J. Cheng, and P. W. Li, Appl. Phys. Lett. **75**, 1051 (1999).
51. W. Li, J. Turpeinen, P. Melanen, P. Savolainen, P. Uusimaa, and M. Pessa, Appl. Phys. Lett. **78**, 91 (2001).
52. A. Markus, A. Fiore, J. D. Ganiere, U. Oesterle, J. X. Chen, B. Deveaud, M. Ilegems, and H. Riechert, Appl. Phys. Lett. **80**, 911 (2002).
53. X. Yang, M. J. Jurkovic, J. B. Heroux, and W. I. Wang, Appl. Phys. Lett. **75**, 178 (1999).
54. D. E. Mars, D. I. Babic, Y. Kaneko, Y. –L. Chang, S. Subramanya, J. Kruger, P. Perlin, and E. R. Weber, J. Vac. Sci. Technol. **B 17**, 1272 (1999).
55. M. Sopanen, H. P. Xin, and C. W. Tu, Appl. Phys. Lett. **76**, 994 (2000).
56. H. P. Xin, K. L. Kavanagh, Z. Q. Zhu, and C. W. Tu, J. Vac. Sci. Technol. **B 17**, 1649 (1999).
57. H. P. Xin, K. L. Kavanagh, Z. Q. Zhu, and C. W. Tu, Appl. Phys. Lett. **74**, 2337 (1999).
58. T. K. Ng, S. F. Yoon, S. Z. Wang, W. K. Loke, and W. J. Fan, J. Vac. Sci. Technol. **B 20**, 964 (2002).
59. S. G. Spruytte, C. W. Coldren, J. S. Harris, W. Wampler, P. Krispin, K. Ploog, and M. C. Larson, J. Appl. Phys. **89**, 4401 (2001).
60. H. P. Xin, C. W. Tu, and M. Geva, Appl. Phys. Lett. **75**, 1416 (1999).
61. Z. Pan, L. J. Li, W. Zhang, Y. W. Lin, R. H. Wu, and W. Ge, Appl. Phys. Lett. **77**, 1280 (2000).
62. see for example "*Semiconductor Quantum Wells and Superlattices for Long-wavelength Infrared Detectors*" edited by M. O. Manasreh (Artech House, Norwood 1993), chapter one, p. 5.
63. E. Tournie, M. –A. Pinault, and A. Guzman, Appl. Phys. Lett. **80**, 4148 (2002).

5. List of publications, professional activities and students:

A. Papers in technical journals and symposia:

1. "*Infrared Optical Absorbance of Intersubband Transitions in GaN/AlGaN Multiple Quantum Well Structures*." Qiaoying Zhou, B. Pattada, Jiayu Chen, M. O. Manasreh, Faxian Xiu, Steve Puntigan, L. He, K. S. Ramaiah, and Hadis Morkoç, J. Appl. Phys. **94**, 10140-10142 (2003) Selected for Virtual Journal of Nanoscale Science & Technology--June 09, Volume **7**, Issue 23 (2003) http://www.vjnano.org

2. "*Optical Absorption of Intersubband Transitions in In0.3Ga0.7As/GaAs Multiple Quantum Dots*." B. Pattada, Jiayu Chen, Qiaoying Zhou, M. O. Manasreh, M. Hussien, W. Ma, and G. J. Salamo, Appl. Phys. Lett. 82, 2509-2511 (2003). Selected for Virtual Journal of Nanoscale Science & Technology--April 21, Volume **7**, Issue 16 (2003) http://www.vjnano.org

3. "*Phonon Modes of GaN/AlN Heterojunction Field Effect Transistor Structures Grown on Si(111) Substrates*." B. Pattada, Jiayu Chen, M. O. Manasreh, S.

Guo, and B. Peres, J. Appl. Phys. **93,** 5824-5826 (2003). Rapid Communication.

4. "*Photoluminescence of Metalorganic Chemical Vapor Deposition Grown GaInNAs/GaAs Single Quantum Wells.*" M. O. Manasreh, D. J. Friedman, W. Q. Ma, C. L. Workman, C. E. George, and G. J. Salamo, Appl. Phys. Lett. **82,** 514-516 (2003).
5. "*Intersubband Transitions in Proton Irradiates InGaAs/InAlAs Multiple Quantum Wells Grown on Semi-insulating InP Substrates.*" Qiaoying Zhou, M. O. Manasreh, B. D. Weaver, and M. Missous, Appl. Phys. Lett. **81**, 3374-3376 (2002).
6. "*Ion-Beam-Produced Damage and its Stability in AlN Films.*" S. O. Kucheyev, J. S. Williams, J. Zhou, C. Jagadish, , M. Pophristics, S. Guo, I. T. Ferguson, and M. O. Manasreh, J. Appl. Phys. **92**, 3554 (2003).
7. "*Response to 'Comment on "Thermal Annealing Efect on the Intersublevel Transitions in InAs Quantum Dots [Appl. Phys. Lett. 78, 2196 (2001)]*"" Y. Berhane, M. O. Manasreh, H. Yang, and G. J. Salamo, Appl. Phys. Lett. **80**, 4869-4870 (2002).

B. Books and Symposia:

1. "**Optoelectronic Properties of Semiconductors and Superlattices.**" A book series edited by M. O. Manasreh (Taylor and Francis, transferred from Gordon and Breach).
   Volume 13: *"III-V Nitride Semiconductors: Optical Properties I."* Volume Editors: H. X. Jiang and M. Omar Manasreh, (Nov 2002).
   Volume 14: *"III-V Nitride Semiconductors: Optical Properties II."* Volume Editors: H. X. Jiang and M. Omar Manasreh, (Nov 2002).
   Volume 16: *"III-V Nitride Semiconductors: Applications and Devices."* Volume Editors: E. T. Yu and M. Omar Manasreh, (January 2003).
   Volume 19: *"III-V Nitride Semiconductors: Growth and Substrate Issues."* Volume Editors: M. Omar Manasreh and Ian Ferguson, (January 2003).
2. "**Progress in Semiconductor Materials II: Electronic & Optoelectronic Applications.**" A symposium is organized by B. D. Weaver, M. O. Manasreh, S. Zollner, and C. Jagadis for the Materials Research Society (Fall 2002).
3. "**Progress in Semiconductor Materials III: Electronic & Optoelectronic Applications.**" A symposium is organized by D. Friedman, M. O. Manasreh, Irina Buyanova, and Danie Auret for the Materials Research Society (Fall 2003).

C. Professional Papers at Regional, National, and International Meetings:

1. "*Intersubband Transitions in InGaAs/InAlAs Multiple Quantum Wells Grown on InP Substrate.*" Qiaoying Zhou, M. O. Manasreh, B. D. Weaver, and M. Missous, Materials Research Society, vol. **744**, 301-307 (2003).

2. "*Normal Incident Infrared Intersubband Transitions of InGaAs/GaAs quantum dots.*" Mohammad Hussein,Wenquan Ma, M. O. Manasreh, and G. J. Salamo, Material Research Society Spring Meeting 2003, Symposium Q (accepted).
3. " *Intersubband Transitions in $In_xGa_{1-x}As/AlGaAs$ Multiple Quantum Wells for Long Wavelength Infrared Detection.*" Clayton L. Workman, Zhiming Wang, Wenquan Ma, Christi E. George, R. Paneer Selvam, Gregory J. Salamo, Qiaoying Zhou, and M. O. Manasreh, Material Research Society, vol. **744**, 607-612 (2003)
4. "*Interband transitions in GaInNAs/GaAs Single Quantum Wells*", M. O. Manasreh, D. J. Friedman, W. Q. Ma, C. L. Workman, C. E. George, and G. J. Salamo, Material Research Society, Material Research Society, vol. **744**, 647-652 (2003)

D. Students supported by the grant:

1. Yosief Berhane (M.S. Student)
2. Jing Chen (Ph. D. student)
3. Qiaoying Zhou (Ph. D. Student)
4. Jiayu Chen (Ph.D. Student)
5. B. Pattada (M. S. Student)